Journal of
Sedimentary
Research

Journal of Sedimentary Research, 2006, v. 76, 633–646
Research Article
DOI: 10.2110/jsr.2006.052

SIGNIFICANCE OF DIFFERENT MODES OF RHIZOLITH PRESERVATION TO INTERPRETING PALEOENVIRONMENTAL AND PALEOHYDROLOGIC SETTINGS: EXAMPLES FROM PALEOGENE PALEOSOLS, BIGHORN BASIN, WYOMING, U.S.A.

MARY J. KRAUS[1] AND STEPHEN T. HASIOTIS[2]
[1] *University of Colorado, Department of Geological Sciences, Boulder, Colorado 80309, U.S.A.*
[2] *University of Kansas, Department of Geology and Natural History Museum and Biodiversity Research Center, Lawrence, Kansas 66045-7613, U.S.A.*
e-mail: Mary.Kraus@colorado.edu

ABSTRACT: **Different modes of preservation of root traces (rhizoliths) provide information on soil-moisture regimes in alluvial paleosols in the Paleogene Fort Union and Willwood formations of the Bighorn Basin, Wyoming, U.S.A. This paper links different styles of rhizolith preservation to paleosols whose other pedogenic attributes provide information on ancient soil drainage. Consequently, the paleodrainage significance of different rhizolith preservation patterns is established more confidently.**

Rhizoliths consisting of elongate gray mottles (rhizohaloes) with red rims are common in relatively well-drained red paleosols. The gray zones are depleted of iron (Fe) whereas the color of the rims indicates hematite accumulation. These features are typical of surface-water gley processes that caused Fe and manganese (Mn) to move from the root channel outward to the soil matrix. Calcareous rhizocretions—either calcareous, tubular concretions or micro-accumulations of carbonate within gray rhizotubules—are also common in moderately well-drained red paleosols.

More poorly drained purple paleosols also have rhizoliths consisting of Fe depletion zones; however, the rhizohaloes are surrounded by yellow-brown (goethite) rims rather than red hematitic rims. In many paleosols, the red and yellow-brown accumulation rims were partly removed by continued depletion, producing abundant irregular-shaped mottles. The nature of the rhizohalo and the color of the Fe-oxide rim provide information about the intensity of gleying that a paleosol underwent. The poorly drained paleosols also show rhizoliths preserved as goethite accumulations contained within gray depletion zones, indicating movement of reduced Fe from the matrix towards the root channel, probably as a result of groundwater-gley processes. The goethite accumulations are intermingled locally with lignite, representing preservation of the root organic material.

Some rhizoliths are preserved as tube-shaped concentrations of small (0.1–0.2 mm diameter) black spheres whose color indicates a mix of Mn and Fe oxides. These are most common in paleosols with low-chroma (gray) matrix colors, indicating very poor drainage. The very poorly drained paleosols also show rhizoliths preserved in jarosite, which is an oxidation product of pyrite.

Careful observational and geochemical analysis of rhizoliths, which are common in continental deposits, can help produce a clearer and more thorough interpretation of ancient drainage conditions. Information about degree of ancient soil wetness or moisture is important for understanding past climatic conditions and for reconstructing terrestrial paleolandscapes.

INTRODUCTION

Root traces or rhizoliths are features commonly described from paleosols and one of the features normally used to recognize paleosols (e.g., Wright 1992; Retallack 2001). The development of rhizoliths indicates the presence of a rhizosphere, which is the area of the soil directly adjacent to and extending several millimeters away from a root. The rhizosphere is the zone most dominated by interactions among the root, the soil, and microorganisms (e.g., Brady and Weil 1999; Violante et al. 2003). In particular, roots and the microbial population associated with them produce organic compounds that affect iron (Fe) and manganese (Mn) in the vicinity of the root (Schwertmann and Taylor 1989; Violante et al. 2003), and many rhizoliths are characterized by the presence of various Fe and Mn minerals. Additionally, roots typically exploit and expand channels or pathways within the soil as they follow the path of least resistance to root growth (e.g., Curl and Truelove 1986). Because those channels provide conduits for water and other soil materials, they also influence the nature of rhizoliths preserved in the paleosol record.

Consequently, rhizoliths show various kinds of preservation patterns including: branching tubes filled by materials (specifically sand, clay, and calcite) that differ in texture and geochemical composition from the surrounding matrix (e.g., Retallack 1983; Elick et al. 1998); elongate and branching gray tubes with rims enriched in Fe and Mn oxides (e.g., Retallack 1983; McCarthy et al. 1998); and, less commonly, strands of carbonaceous material (e.g., McSweeney and Fastovsky 1987). Some of these rhizoliths provide information on the hydrologic regime of the ancient soil. For example, rhizoliths preserved as elongate gray tubes with

1527-1404/06/076-633/$03.00

Fe-rich rims are redoximorphic features that indicate seasonal saturation and the filling of root channels with water (e.g., Vepraskas 1994; PiPujol and Buurman 1994). Other kinds of rhizoliths are connected less confidently to particular drainage conditions.

The goal of this paper is to expand the utility of rhizolith morphologies for interpreting ancient soil-moisture regimes by linking different kinds of rhizolith preservation to paleosols whose other attributes provide information on drainage conditions prevalent at the time of rhizolith development. Paleosols formed on fluvial strata of the Paleogene Fort Union and Willwood formations show varying degrees of soil-moisture regimes, and those different kinds of paleosols are characterized by different rhizolith morphologies. Here, we describe three different kinds of paleosols: moderately drained red paleosols, imperfectly to poorly drained purple paleosols, and very poorly drained gray paleosols. Each of these paleosols is characterized by rhizoliths that show contrasting modes of preservation that distinguish the soil-moisture regimes interpreted from biogenic and physicochemical characteristics.

This paper also modifies the classification of Klappa (1980), which applied the term rhizolith to all trace fossils of roots. We introduce a new term—rhizohaloes—to describe Fe- and Mn-depleted areas that formed around roots as a result of fluctuating soil-moisture and decay of the root. Rhizohaloes are a type of root trace that could not be recognized if it were not for color variations in the paleosol.

Interpreting ancient soil-moisture regimes is important for understanding past climatic conditions. It is also important for reconstructing ancient alluvial landscapes because the spatial distribution of paleosols of different drainages reflects, in part, the particular landforms on which they developed (e.g., Kraus 1999).

DEFINITION OF RHIZOLITHS

Klappa (1980) defined rhizoliths as organosedimentary structures that preserve the activity of roots of higher plants. Rhizoliths were recognized as the products of subaerial exposure and pedogenesis (Sarjeant 1975; Klappa 1980). More recently, they have been recognized as trace fossils that preserve plant-substrate interactions and that indicate the relative position of the vadose or phreatic zones (Retallack 2001; Hasiotis 2002, 2004). Nonetheless, the terminology describing root trace fossils is confusing. If original organic materials are present, the root traces are considered body fossils by some workers (e.g., Ekdale et al. 1984). Even if no organic material is present, other workers consider the overall root pattern as part of the plant body because plants do not engage in locomotion, dwelling, feeding, and resting, which are animal behaviors generally regarded as producing traces and trace fossils (e.g., Sarjeant 1975; Klappa 1980; Ekdale et al. 1984).

The structures and patterns produced by roots indicate activity and behavior over the lifetime of the plant (Sarjeant 1975). The patterns produced by roots represent the search for interstitial water and minerals by the plant via its root system; this is plant behavior. Consequently, roots leave trace fossils behind. The presence of a plant body fossil within its trace fossil is analogous to finding a crayfish fossil in its burrow (Hasiotis and Mitchell 1993) or a therapsid fossil in its helical burrow (Smith 1987). The rhizoliths or burrows are still trace fossils, although, in some examples, the tracemaker is preserved with it trace fossil (Sarjeant 1975; Klappa 1980). Rhizoliths are original cellular material, mineral replacements, or mineral impregnations that preserve anatomical features of the root (Klappa 1980).

In this paper, we slightly modify the terminology proposed by Klappa (1980). The term rhizolith is retained as a general descriptor for all trace fossils of roots, even if original plant material is preserved within the structure. Rhizoliths include Klappa's root molds and root casts, where the mold is the void left behind by a decayed root and the cast is the sediment or cement that fills the mold. Following Klappa, rhizotubules are cemented cylinders around root molds that can fill later with sediment. Minerals that accumulate as concretions or nodules around a living or dead root are termed rhizocretions. Finally, we introduce the term rhizohalo to describe the Fe- and Mn-depleted zone that forms around a root due to fluctuating soil moisture levels and attendant decay of the root. Without the depletion zone, the trace of the root is not visible because no true mold or cast of the tubular structure is otherwise preserved.

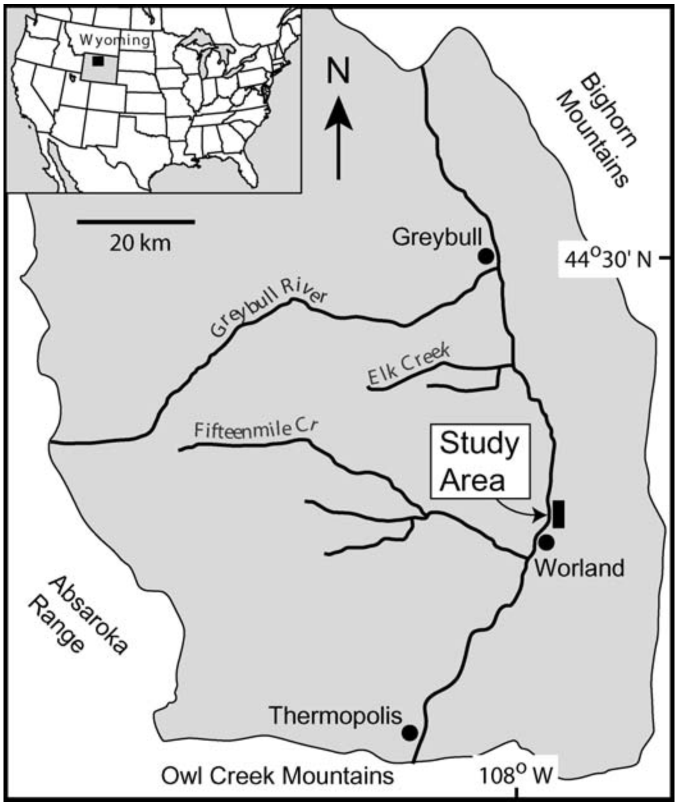

FIG. 1.—Map of the Bighorn Basin (shaded) showing location of the study area in McDermotts Butte and mountains surrounding the basin. Beartooth Mountains lie northwest of the basin and are not shown. Modified from Davies-Vollum (2001). Inset map shows location of Bighorn Basin in northern Wyoming.

GEOLOGICAL SETTING

The Willwood Formation consists of alluvial strata that accumulated during latest Paleocene and early Eocene time in the Bighorn Basin. The underlying Paleocene Fort Union Formation is more widely exposed across the northern Rocky Mountain area. This study focuses on exposures of the uppermost Fort Union Formation and lowermost Willwood Formation in the McDermotts Butte area of the Bighorn Basin (Fig. 1). Here, both formations consist of alluvial strata for which the main sources of sediment were the surrounding Bighorn, Beartooth, and Owl Creek mountain ranges, which formed during the latest Cretaceous through late Paleocene Laramide orogeny (Neasham and Vondra 1972; Bown 1980). Most orogenic uplift of these ranges had ceased prior to Willwood deposition (Omar et al. 1994). The basin is bounded to the west by the Absaroka volcanic complex, which formed after deposition of the Willwood Formation (Bown 1980). The basin was open and drained to the north.

The paleosols that are the focus of this study formed during and immediately prior to the Paleocene–Eocene thermal maximum (PETM). The PETM was a dramatic, ephemeral (~ 100,000 yr) global warming event that occurred at the Paleocene–Eocene boundary (e.g., Kennett and Stott 1991; Zachos et al. 1993). Climate during deposition of the study section was generally subtropical with seasonal rainfall (Wing 1981; Wing and Greenwood 1993). Leaf-margin analysis of paleofloras shows that, over the last ~ 1 million years of the Paleocene, MAT rose from ~ 13°C to over 15°C and reached 18°C during earliest Eocene time, when Willwood strata at McDermotts Butte were deposited (e.g., Bao et al. 1999; Wing et al. 2000).

METHODS

Morphologic features of the paleosols, including colors, nodule type, and grain size, were described in the field. Colors were described from fresh, dry samples. Field descriptions of the rhizoliths include morphology, size, color(s), lithology, and nature of the enclosing matrix. Each paleosol field unit and its contained rhizoliths were also described in the laboratory using a binocular microscope. Thin sections of representative samples of paleosol units and rhizoliths were examined for micromorphologic features.

Major oxide weight percents of representative paleosol samples were determined using X-ray fluorescence (XRF) of powdered whole-rock samples. X-ray diffraction (XRD) was used to evaluate the mineralogy of the different colored paleosol units and rhizoliths. Samples of particular colors were hand picked from paleosol units and rhizoliths. Powdered samples were analyzed using a Scintag X-ray diffractometer with a Cu target. Although XRD analysis of iron oxides in soils is difficult because they are generally present in only small amounts, hematite and goethite could be detected by using a slow scan rate (0.5° per minute). Samples of particular nodules were analyzed using a Jeol JXA-733 electron microprobe equipped with five wavelength-dispersive spectrometers and a Tracor Northern energy-dispersive spectrometer.

PALEOSOL CATEGORIES

The Fort Union and Willwood formations are mudrock-dominated alluvial successions that contain moderately to strongly developed paleosols (e.g., Kraus and Aslan 1993; Kraus 1998). Paleosols in the study area show colors and other morphologic features that allow them to be subdivided into three kinds of paleosols based on estimated soil-moisture regime: moderately well drained, imperfectly to poorly drained, and very poorly drained. These categories are based on observations from the Willwood and Fort Union formations. Other classes probably exist in formations found in other alluvial basins.

In general, Willwood paleosols are dominated by red, yellow-brown, and purple as matrix and mottle colors, where matrix color is the dominant color of a bed, and mottles are small areas of a different color (e.g., Sprecher 2001). In contrast, uppermost Fort Union paleosols are characterized by gray and purple colors. We refer to colors by name in this discussion, but specific Munsell color assignments for color name are in Table 1.

Soil colors are related to the presence and absence of particular iron oxides. Red and yellow-brown colors result from a mix of hematite (Fe_2O_3) and goethite ($FeO(OH)$), and, as hematite increases, color becomes redder (e.g., Schwertmann and Taylor 1977; Scheinost and Schwertmann 1999; Cornell and Schwertmann 2003). Purple colors in sedimentary rocks have also been attributed to the presence of hematite (e.g., McBride 1974; Blodgett 1988; Wright et al. 2000). Gray generally reflects the absence of iron oxide minerals (e.g., Vepraskas 1994; PiPujol and Buurman 1994).

TABLE 1.—*Typical Paleosol Colors.*

Descriptive color name	Munsell hue, value, chroma
Red	Hues of 5R and 10R; 5R 3/4 (dusky red) and 10R 3/4 (dark reddish brown) common
Yellow-brown	10YR 5/4 (Moderate yellow-brown) to 10YR 6/6 (dark yellowish orange)
Purple	Hues of 5P and 5RP with values and chromas of 6/2 to 4/2
Gray	5Y 8/1 (Yellowish gray) to 5Y 6/1 (light olive gray) 5Y4/1 (Olive gray) 5GY 8/1 to 6/1 (Light greenish to greenish gray)

Although workers such as Retallack (1991) and Blodgett et al. (1993) have attributed reddening to recrystallization of iron oxides during post-burial diagenesis, the mix of yellow-brown (goethite) and red (hematite) colors suggests that diagenesis has not greatly impacted color in the paleosols. As PiPujol and Buurman (1994) pointed out, diagenesis should have affected all iron oxides in a similar way rather than producing a mix of hematite and goethite. Furthermore, mottle patterns are similar to those found in modern soils, also suggesting they are not diagenetic in origin (PiPujol and Buurman 1994).

Moderately Well Drained Paleosols

Many Willwood paleosols consist of a red mudstone or silty mudstone that is overlain by a gray or yellow-brown mudstone (Fig. 2). The red mudstone grades downward into gray units, showing only weak pedogenesis, that form the base of the profile. Yellow-brown mottles or masses *sensu* Vepraskas (1994), most of which are several millimeters to 1 cm in diameter, are common in the red beds. Gray haloes surround the yellow-brown masses in some red beds. Many red mudstones contain carbonate nodules and slickensides, which are found as shiny, clay-lined fractures that intersect to form concave-up, dish-shaped structures.

The yellow-brown horizon seen at the top of the section in Figure 2 is interpreted as the A horizon and the underlying red bed as the B horizon of the paleosol, with the unit containing carbonate nodules designated a Bk horizon. The red color indicates the presence of hematite, which is confirmed by XRD analysis (Table 2). Hematite and the local presence of carbonate nodules imply that the B horizon was at least moderately well drained and oxidized (e.g., Kampf and Schwertmann 1982; Schwertmann 1993). Yet, the yellow-brown masses in the B horizon and the yellow-brown color of the A horizon indicate that red soils underwent seasonal wetting and drying. Red soils in the tropics and subtropics commonly have a yellow A horizon above a red B horizon (e.g., Kampf and Schwertmann 1982), and the yellow-brown colors are characteristic of red soils with intermediate drainage (Macedo and Bryant 1987). Macedo and Bryant (1987, 1989) attributed this phenomenon to the selective dissolution of hematite caused by weak reduction related to seasonal wetness and the high organic content and roots in the upper part of the profile. Following Stolt et al. (1994), the yellow-brown masses might indicate that hematite was removed preferentially from some areas of the B horizon, leaving behind only goethite. Local removal of hematite, but not goethite, indicates weakly reducing conditions, generally in the presence of organic matter, and suggests that periods of seasonal wetting were short (e.g., Macedo and Bryant 1989; Stolt et al. 1994). The presence of slickensides is consistent with seasonal wetting and drying of this kind of paleosol (e.g., Wilding and Tessier 1988). Based on the red colors of the B horizon, the presence of distinct yellow-brown masses, and local presence of carbonate nodules, this kind of paleosol is regarded as moderately well drained (Landon 1984).

Imperfectly to Poorly Drained Paleosols

A purple paleosol profile from the transition between the Willwood and Fort Union formations is representative of imperfectly to poorly drained paleosols. The profile consists of a gray mudrock above a purple

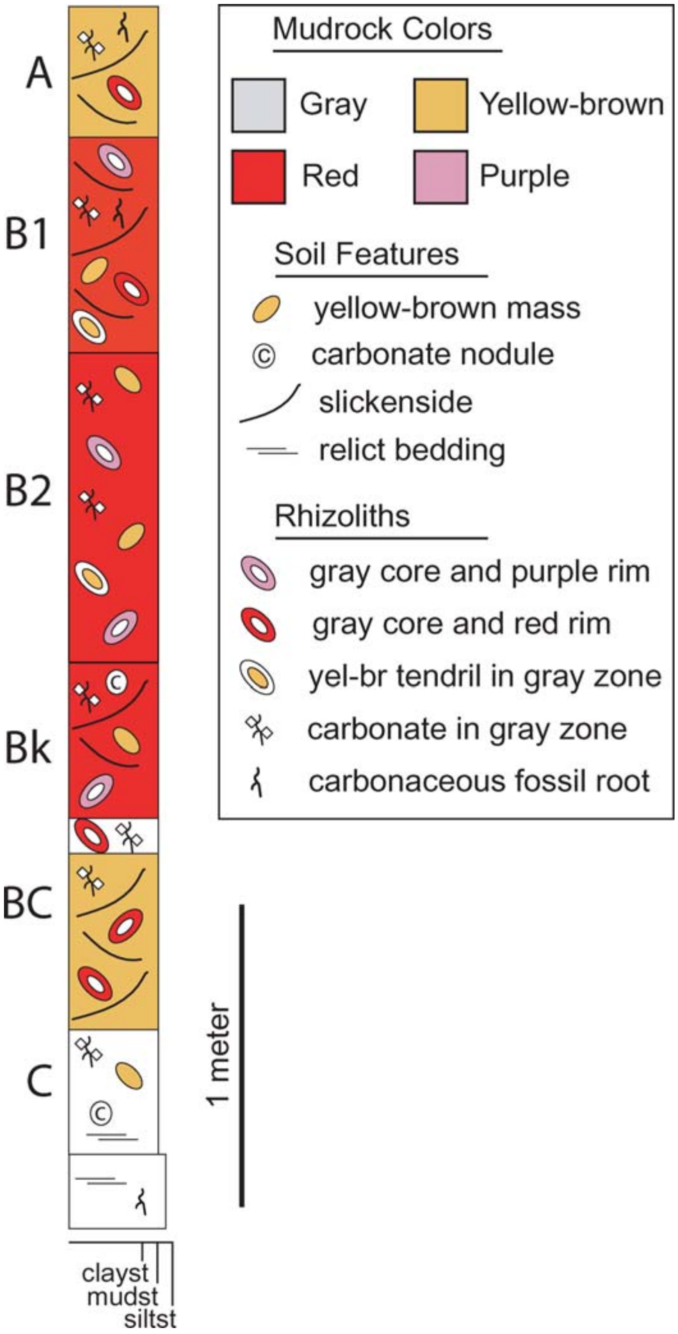

FIG. 2.— Detailed measured section through an example of a moderately well-drained paleosol (red paleosol in the Willwood Formation) illustrating pedogenic features and different kinds of rhizoliths. A = A horizon; B1 and B2 indicate subdivisions of the B horizon based on different morphologic attributes; Bk = calcic B horizon; C = C horizon.

mudstone or claystone that grades down into gray mudrocks (Fig. 3). Both the gray and purple beds contain yellow-brown masses. A small percentage of the masses (5 to 10%) are in the form of small (< 3 mm diameter) nodules that XRD analysis shows contain goethite (Kraus and Aslan 1993). Yellow-brown masses in the purple matrix are generally embedded within gray depletion zones. Red mottles with distinct boundaries are present locally in purple beds. Carbonate is generally absent from the purple paleosols. Large slickensides are found in both purple and gray beds.

TABLE 2.—*XRD results showing iron oxides identified in paleosol horizons and rhizohalo rims of different colors.*

Sample	Color	Hematite	Goethite
97-1-11	Red matrix	Yes	No
03-6-2R	Red matrix	Yes	Yes
MB05-2-2	Red rim	Yes	No
MB03-4-2R	Red rim	Possible trace	Possible trace
Root R	Red rim	Possible trace	No
87-6-7	Purple matrix	Yes	Yes
MB03-6-2P	Purple matrix	??	No
MB04-3-5P	Purple matrix	??	No
MB-05-6-4	Purple matrix	Yes	Yes
MB04-3-5YB	Yellow-brown matrix	No	Yes
MB04-3-1YB	Yellow-brown rim	No	Yes
MB05-6-4YB	Yellow-brown rim	No	Yes
MB05-3-5YB	Yellow-brown rim	No	Yes

Thin-section observations suggest that purple mudstones are depleted in Fe compared to red mudstones. Thin sections show that purple matrix is characterized by widely dispersed red microspheres < 5 µm in diameter, whose color indicates that they consist of hematite. In contrast, the red masses are so heavily stained with red that individual spheres

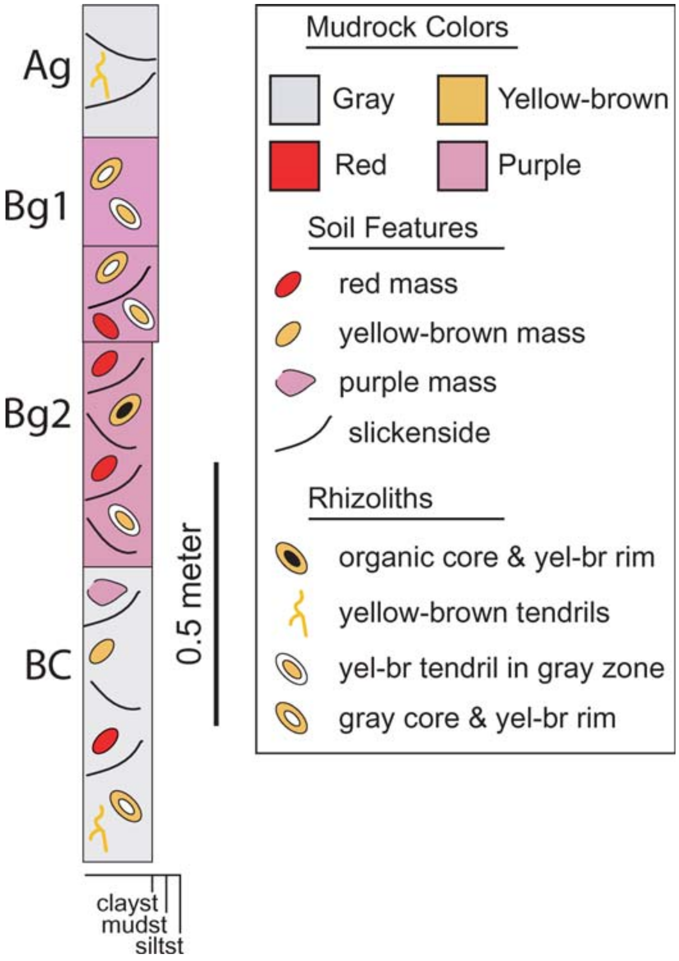

FIG. 3.— Detailed measured section through an example of an imperfectly to poorly drained paleosol (purple paleosol in the transition zone between the Willwood and Fort Union formations) illustrating pedogenic features and different kinds of rhizoliths. Ag = gleyed A horizon; Bg1 and Bg2 = gleyed subdivisions of the B horizon; BC = transitional between a B and C horizon.

cannot be distinguished. Iron depletion is confirmed by XRF analysis, which shows that the average Fe_2O_3 wt% of red mudstones is 6.95% ($n = 42$), whereas purple mudstones contain, on average, 5.86 wt% Fe_2O_3 ($n = 19$). In addition, the purple mudstones are depleted in MnO_2, with the average for purple beds 0.008 wt% and for red beds 0.023 wt%.

The purple interval is interpreted as a B horizon with the overlying gray bed representing an A horizon. The yellow-brown nodules are similar to those in near-surface horizons of imperfectly to poorly drained modern soils (e.g., Ransom et al. 1987; Griffin et al. 1992). In addition, the gray depletion zones that surround the yellow-brown mottles and nodules are common in imperfectly to poorly drained soils (e.g., Ransom et al. 1987). The observed depletion of Fe and Mn suggests that both were reduced and removed from the purple beds.

Thus, the presence of purple rather than red soil matrix and the absence of carbonate indicate that this kind of soil was less well drained than red paleosols in the Willwood Formation. In addition, the presence of yellow-brown masses in the A horizon and distinct yellow-brown and gray mottles in the purple B horizon indicate that purple paleosols were imperfectly to poorly drained (Landon 1984). Because gleying was important, the B horizon is interpreted as a gleyed B (Bg) horizon and the overlying A is an Ag horizon.

Very Poorly Drained Paleosols

Two representative sections from the uppermost part of the Fort Union Formation illustrate the very poorly drained paleosols (Fig. 4). One consists of gray mudstones that coarsen downwards to gray siltstones with relict bedding (Fig. 4A). XRF analysis shows that gray beds contain less Fe_2O_3 (5.29 wt%; $n = 58$) than beds of any other color. Yellow-brown masses are present locally in the gray beds as are gypsum crystals and yellow (5Y 7/6), powdery nodules that microprobe and XRD analyses indicate consist dominantly of jarosite ($KFe_3(SO_4)_2(OH)_6$). Slickensides are common in the finer-grained beds. Thin sections show abundant fine organic debris scattered through the rock.

The second section also consists of gray mudstones and silty mudstones that can be subdivided into several paleosol profiles (Fig. 4B). Neither jarosite nor gypsum is present in this section, and yellow-brown masses are uncommon. Distinctive black nodules that are vertical to subvertical cylinders with diameters and heights of several tens of centimeters are present at the top of the section and at other stratigraphic levels in the uppermost Fort Union Formation in the study area.

The pervasive reduced (gray) matrix colors, abundant organic fragments, and local presence of jarosite and gypsum indicate very poorly drained conditions (e.g., Kraus 1998). The paleosols underwent gleying during which Fe was removed from the reduced (gray) matrix and then reprecipitated in better oxidized areas within peds or along ped faces and soil channels as yellow-brown masses (e.g., Duchaufour 1982; Vepraskas 1994). The XRF results confirm that Fe was depleted from the gray matrix. The presence of jarosite and gypsum are consistent with the poorly drained nature of the paleosol. Jarosite commonly forms from pyrite when a water-logged soil is drained and oxidized (e.g., van Breeman 1975; Miedema et al. 1986). Oxidation of pyrite can also produce iron oxides and gypsum (e.g., Van Breeman 1982; Dent 1986), both of which are associated with the jarosite. In addition to waterlogged conditions, pyrite precipitation requires abundant organic matter to furnish sulfate-reducing bacteria with an energy source (e.g., Berner 1984; Rabenhorst and Haering 1989).

RHIZOLITHS

Moderately Well Drained Paleosols

Two kinds of rhizoliths are most characteristic of the red paleosols: elongate, gray mottles with red or purple rims and calcareous accumulations (Fig. 2). Rhizoliths with carbonaceous material or preserved as yellow-brown tendrils are present but sparse. Those features are more typical of more poorly drained paleosols and are described later.

Depletion Zones.—Elongate gray mottles that taper and branch downwards and that have approximately circular cross sections are common (Fig. 5). Many gray mottles have distinct red rims or hypocoatings (*sensu* Bullock et al. 1985) (Fig. 5A, B). In some examples, the rims are purple or the red rims are separated from the inner gray core by a purple rim (Fig. 5C, D). Thin sections show that the red rims are characterized by densely packed, small (< 0.1 mm), subspherical red particles whereas the red particles are absent or only locally scattered in the gray areas (Fig. 5E). The red spheres are widely scattered through the purple borders. XRD analysis shows that hematite is present in the red rims (Table 2). Some gray zones contain black organic fragments or strands, which are visible both in hand sample and thin section (Fig. 5F).

The gray mottles can be large, with diameters up to 30 cm and subvertical lengths up to 100 cm. These large examples have a true vertical dimension of at least 60 cm, which is the thickness of the red B horizon they penetrate. They also have secondary and tertiary gray rhizoliths extending from them.

The elongate, branching nature of the gray mottles and their circular cross sections indicate that these mottles were produced by roots; thus, they are rhizohaloes as defined above. The colors associated with the traces are typical of redoximorphic features that are present in modern soils from changes in the redox conditions in response to fluctuations in degree of saturation (e.g., Vepraskas et al. 1992; Vepraskas 1994). The gray zones with tubular shape are Fe depletions that formed when the soil was saturated and relatively depleted of oxygen (O_2), Fe was reduced and subsequently removed from areas of the soil matrix (e.g., Duchaufour 1982; Fanning and Fanning 1989). Iron reduction is common adjacent to roots, especially under surface-water gley conditions. In O_2-starved conditions induced by stagnating water that filled the root channel, microbial communities utilize Fe(III) as the electron receptor in their metabolic pathways as they degrade organic matter, in this case decaying roots (e.g., Schwertmann and Taylor 1989; Violante et al. 2003). The localized reduction and leaching of soluble Fe(II) is facilitated by this process, and Fe is translocated outward from the root channel and precipitated where conditions were more oxidizing to form the Fe(III) oxide rim.

The presence of Fe concentrations in the matrix around gray depleted zones (rhizohaloes) is indicative of surface-water gleying caused by perched water tables (e.g., Fanning and Fanning 1989; Vepraskas et al. 1992). PiPujol and Buurman (1994) recognized various stages of surface-water gleying based on features of gray depletion zones and their hypocoatings. Early gley stages show only incipient development of bleached zones and faint Fe-rich rims around those. As gleying continues, the bleached zones enlarge and the red rims intensify. Eventually, the depletion channels have expanded to the point that the Fe-rich rims show significant dissolution, which is probably what causes the purple inner ring and outer red ring associated with some rhizohaloes. With even further iron removal, only a purple rim remains around the gray depletion channel. Consequently, close inspection of the rhizohaloes and their Fe-oxide rims provides information about the intensity of the gleying that an ancient soil underwent.

Calcareous Accumulations.—Some gray rhizohaloes contain powdery calcium carbonate or carbonate nodules (Figs. 2, 5G). Even when not visible in the field or hand samples, thin sections show the local presence of micro-accumulations of calcite within some gray rhizohaloes (Fig. 5H). Most consist of micrite or microspar with crystal sizes of ~ 0.05 mm, although some examples have coarser spar in the center of the

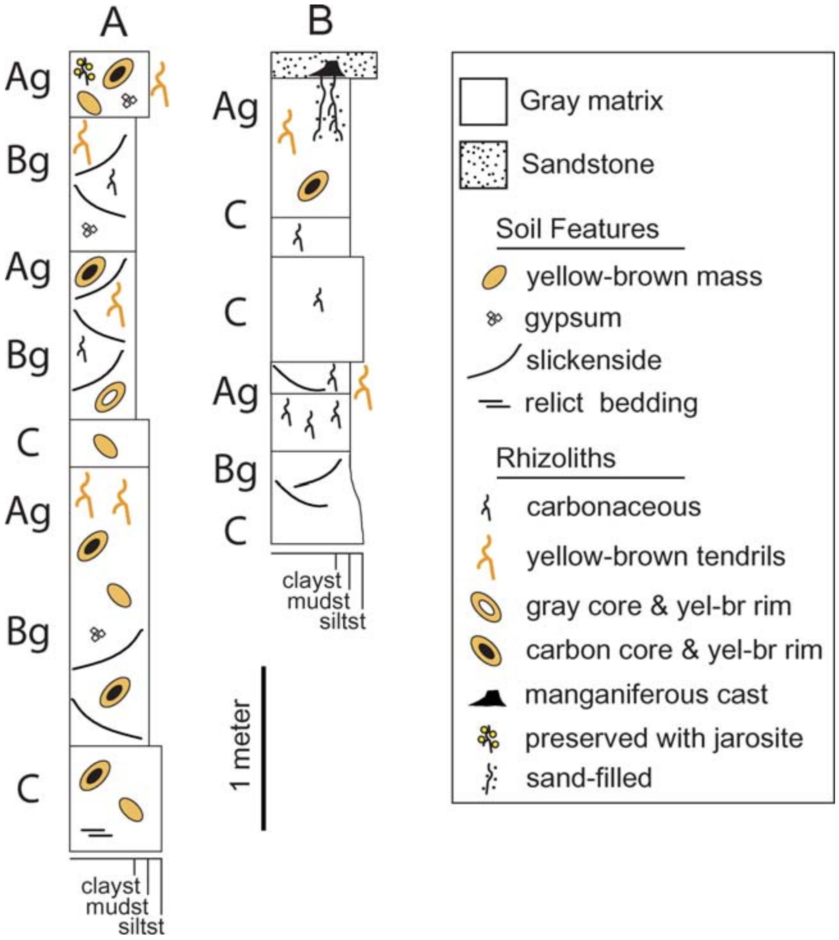

FIG. 4.—Detailed measured sections through two very poorly drained paleosol sections (uppermost Fort Union Formation) illustrating paleosol features and different kinds of rhizoliths. **A)** Gray paleosol section that contains local jarosite and gypsum. **B)** Gray paleosol section that contains cylindrical black nodules. Ag = gleyed A horizon; Bg = gleyed B horizon; C = C horizon.

accumulation. Many micro-accumulations have long dimensions < 1 mm.

The development of calcite associated with roots and root channels has been documented by numerous workers (e.g., Klappa 1980; Cohen 1982). Cohen (1982) attributed formation of such rhizogenic calcite to development of a soil channel following decay of the root. Calcite can precipitate in the channel from fluids moving through it, and cementation can extend outwards from the channel to the surrounding soil. Calcitic rhizoliths are common in regions where evapotransportation is greater than effective precipitation (e.g., Brady and Weil 1999); however, micritic nodules precipitated around root pores have also been observed in soils of the Mississippi River floodplain, where annual rainfall is relatively high (150 cm) (Farrell 1987; Aslan and Autin 1998). Thus, the key to forming calcite in and around root channels appears to be episodic drying of the soil for a sufficiently long period.

The microscopic accumulations within the gray rhizohaloes are interpreted as rhizocretions that precipitated as pedogenic mineral accumulations around the root and fine root hairs. The microscopic accumulations within the gray rhizohaloes resemble the type C6 calcite accumulation of PiPujol and Buurman (1997), which they attributed to formation in seasonal climates during the dry season. Episodic rains introduce water into the soil channels, and, if the water contains easily solubilized calcium carbonate, micrite precipitates when the soil dries.

A diagenetic origin for the calcite is unlikely because its presence is closely linked to the type of paleosol. Whereas a red paleosol generally contains calcite associated with at least some of its gray rhizohaloes, an overlying or underlying purple paleosol lacks the calcareous accumulations. Diagenesis should not have preferentially affected only gray rhizohaloes in red paleosols.

Imperfectly to Poorly Drained Paleosols

Like the red paleosols, the imperfectly to poorly drained paleosols contain numerous gray rhizohaloes with iron oxide hypocoatings;

→

FIG. 5.—Rhizoliths from moderately well-drained red paleosols. **A)** Field photo of gray rhizohaloes with red rims. Yellow-brown mudstone in lower part of paleosol shown in Figure 2. Lens cap is 64 mm in diameter. **B)** Close-up of rhizohaloes in Part A showing finer rhizohaloes extending from larger ones and good examples of red rims (yellow arrows). **C)** Field photo of branching, gray rhizohaloes with purple rims (yellow arrows); red B horizon. **D)** Close-up of gray rhizohalo (black arrow) with purple rim (yellow arrow); red B horizon. **E)** Photomicrograph of gray rhizohaloes with red rims (black arrows). Gray rhizohaloes are depleted of red Fe oxides, which are concentrated in the red rims (combined plane and reflected light). **F)** Gray rhizohaloes surrounding black, carbonaceous root fossils (arrows) from the red paleosol. **G)** Field photo of purple-rimmed, gray rhizohaloes with carbonate accumulations interpreted as rhizocretions (arrows). **H)** Photomicrograph of carbonate rhizocretions (arrows) within a gray rhizohalo surrounded by a red rim (combined plane and reflected light).

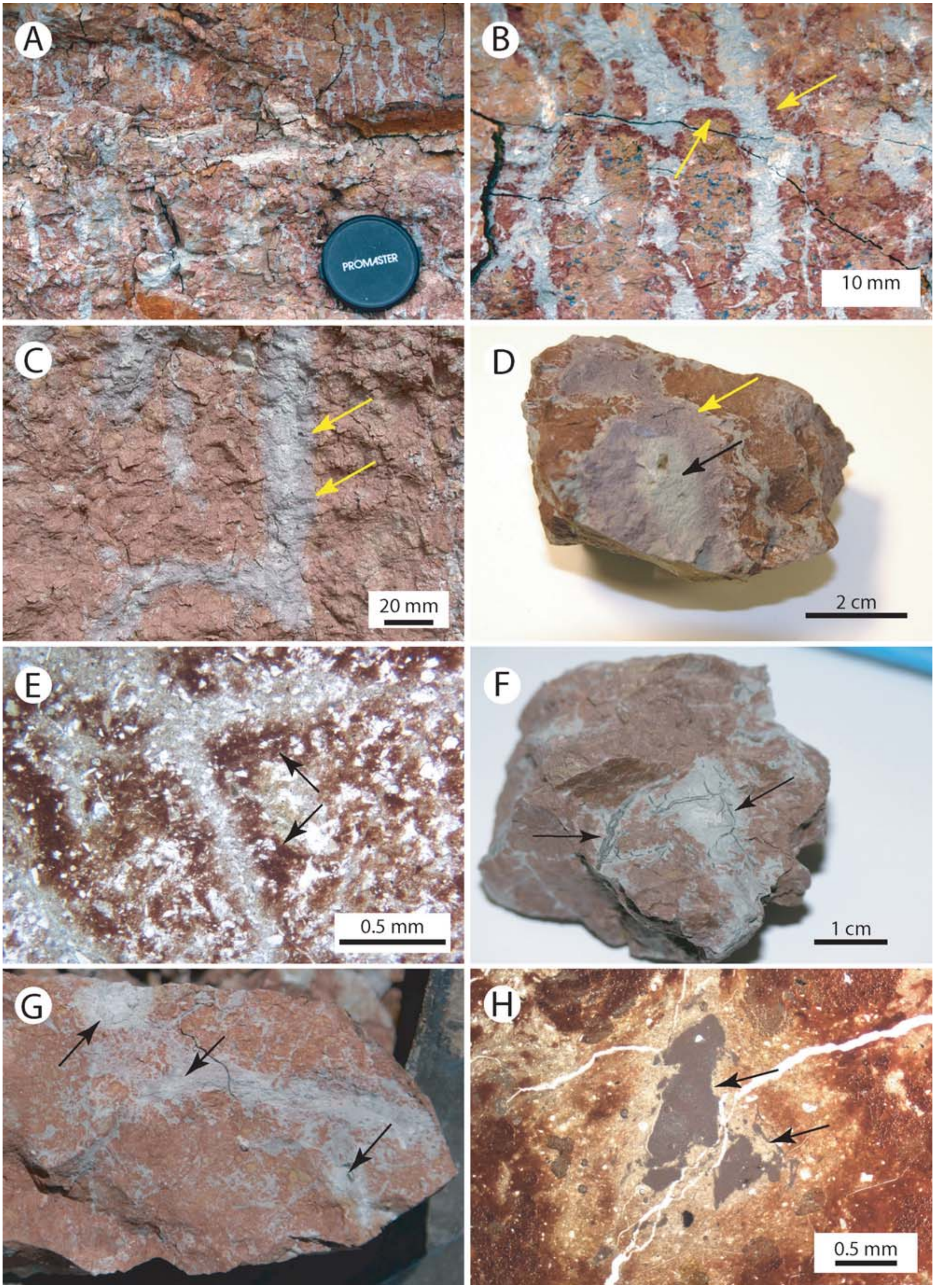
A
PROMASTER
B
10 mm
C
20 mm
D
2 cm
E
0.5 mm
F
1 cm
G
H
0.5 mm

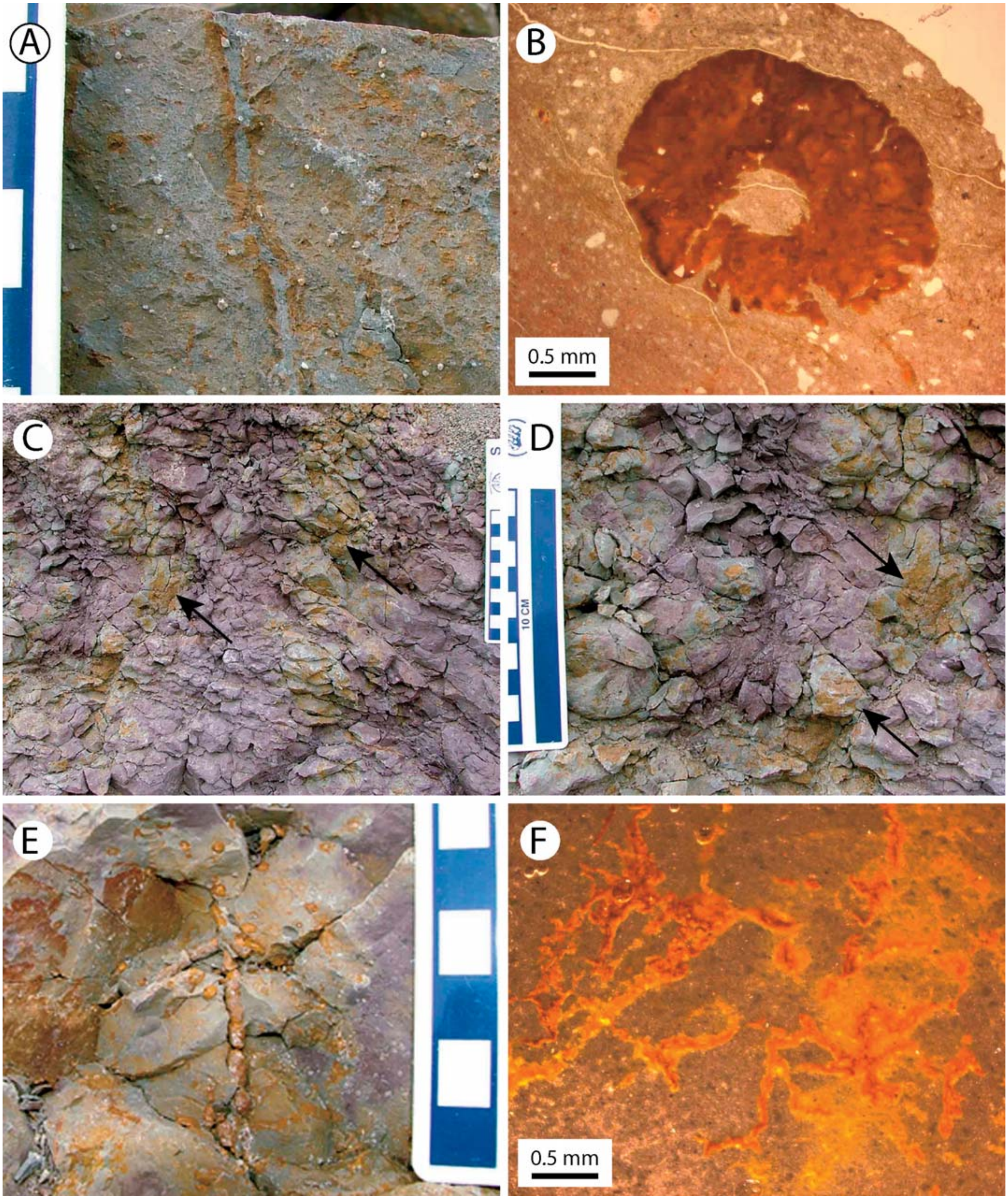
A
B
0.5 mm
C
D
10 CM
E
F
0.5 mm

however, the major Fe-oxide color is yellow brown (Fig. 3). Also common are rhizoliths preserved as yellow-brown accumulations within gray depletion channels. Carbonaceous material is variably present; carbonate was not observed.

Depletion Zones with Yellow-Brown Rims.—Gray rhizohaloes are present in the purple paleosols and stand out because they have yellow-brown rims (Fig. 6A). In some cases, the yellow-brown impregnation is so intense that Fe-oxide tubes formed around the gray depletion zone to produce rhizotubules (Fig. 6B). Individual yellow-brown rhizotubules have outside diameters up to 3.6 mm and inside diameters up to 1.4 mm.

The yellow-brown rhizotubules are a kind of redox concentration or hypocoating. As with the red-rimmed gray depletion zones, the gray core was a zone where Fe was reduced and removed. The Fe-oxide rim was an area where Fe accumulated because conditions were more strongly oxidizing. The yellow-brown color and XRD analyses (Table 2) indicate that the Fe oxide is goethite, whose formation is favored over hematite in soils with higher contents of soil moisture and organic matter (e.g., Kampf and Schwertmann 1982; Schwertmann and Taylor 1989). Goethite tends to form in soils that remain relatively wet for longer periods than in soils in which hematite is found (e.g., PiPujol and Buurman 1994).

Like the gray depletion zones with hematitic rims, these probably indicate surface-water gleying. The presence of goethite hypocoatings associated with rhizoliths indicates soils that were less well drained than those dominated by rhizoliths with red (hematite) hypocoatings (e.g., PiPujol and Buurman 1994).

Yellow-Brown Accumulations in Gray Depletion Zones.—The imperfectly to poorly drained paleosols also contain yellow-brown (goethite) accumulations within gray depletion zones and within gray beds (Fig. 6C). Some of the depletion zones are vertical to subvertical, elongate gray areas that extend downwards up to 30 cm. The yellow-brown accumulations vary from masses that are weakly impregnated with goethite to rhizocretions that are more heavily cemented with Fe oxide and have sharp boundaries (Fig. 6D, E). Thin sections also show the presence of thin (0.01 to 0.02 mm thick), branching, yellow-brown tendrils that can be traced for up to several millimeters (Fig. 6F). The yellow-brown accumulations are intermingled locally with lignitic material.

The gray depletion zones are rhizohaloes that contain yellow-brown masses interpreted as rhizocretions. The yellow-brown accumulations within gray rhizohaloes indicate that dissolved Fe diffused from the matrix towards the root channel, where it precipitated as goethite (e.g., PiPujol and Buurman 1994; Sundby et al. 1998). This kind of morphology has been associated with soil matrix that remains wet long enough for reducing conditions to be maintained (e.g., Vepraskas et al 1992; PiPujol and Buurman 1994). With the growth of plants, roots penetrate the soil and form channels along which air can enter and create zones of oxidation. Rhizocretions like these are known also to form in marshes where hydrophytic plants transport O_2 to the sediment through highly porous tissues termed aerenchyma (e.g., Sundby et al. 1998; Sundby et al. 2003). The carbonaceous cores to some traces represent preservation of the root organic material within the rhizolith.

Very Poorly Drained Paleosols

Carbonaceous strands preserved within rhizoliths—body fossils within their traces—are common in the very poorly drained paleosols, whereas gray rhizohaloes with Fe-oxide hypocoatings are sparse. Rhizoliths preserved with Fe and Mn oxides and jarosite also characterize the poorly drained paleosols.

Iron-Oxide Rhizoliths.—Some rhizoliths are preserved as yellow-brown tendrils within the gray paleosol matrix (Fig 7A). Similarly to the purple paleosols, thin sections show thin (0.01 to 0.02 mm thick), branching, yellow-brown strands that are vermiform in shape (Fig. 7B). The tendrils have sharp contacts with the surrounding matrix, and, locally, some of them contain a darker core that higher magnification shows to be red microspheres (0.01 mm diameter) whose color suggests they contain hematite (Fig. 7B). A few tendrils are entirely red, signifying the presence of hematite as well as the probable presence of goethite (red colors generally indicate hematite in addition to goethite; e.g., Schwertmann 1993).

The yellow-brown tendrils are interpreted as rhizocretions of fine roots. They resemble those found in the purple paleosols and indicate that the soil matrix was sufficiently wet (and anoxic) to reduce and solubilize Fe, which then diffused towards the root channel and precipitated as goethite (e.g., PiPujol and Buurman 1994; Sundby et al. 1998). Brady and Weil (1999) concluded that reddish zones associated with root channels in a gray matrix are produced only by wetland plants that have aerenchyma from which O_2 can diffuse into the soil. Thus, the red tendrils signify poorly drained soil conditions.

Carbonaceous Root Fossils within Rhizoliths.—Although black carbonaceous strands are found in the relatively well drained and imperfectly to poorly drained paleosols, they are more common in the very poorly drained paleosols. Furthermore, they are generally found in gray matrix rather than within gray rhizohaloes surrounded by Fe-oxide hypocoatings (Fig 5, 7C). Iron oxide, in the form of goethite on the basis of its yellow-brown color, may be associated with the carbonaceous material. The best example of a carbonaceous root fossil is oriented vertically and has a preserved length of 3.5 cm (Fig. 7C). This primary carbonaceous root gives rise to first-order and second-order lateral roots.

The preservation of organic matter is controlled by rapid burial or anoxic conditions (e.g., McCabe and Parrish 1992). Because roots are already below the soil surface, the key to the preservation of carbonaceous roots is anoxic conditions resulting from high water tables. Other examples of well-preserved carbonaceous root fossils are also described mainly from what are interpreted as hydromorphic paleosols (e.g., McSweeney and Fastovsky 1987; McCarthy et al. 1998).

Jarosite.—Powdery, yellow (10YR 8/6) spheres generally less than 2 mm in diameter are found in several beds within one of the representative poorly drained paleosols (Fig. 4A). Although some are scattered through the matrix, most spheres are grouped to form elongate, branching structures (Fig. 7D). XRD and microprobe analyses shows that the spheres consist chiefly of jarosite with lesser amounts of gypsum and native sulfur. In thin section, reflected light also shows spherical to

←

FIG. 6.—Rhizoliths in poorly drained paleosols. **A)** Field photo of gray rhizohalo with yellow-brown rim. Gray mudstone in moderately poorly drained paleosol shown in Figure 3. Scale shows centimeter markings. **B)** Photomicrograph of yellow-brown (goethite) rhizotubule seen in cross section from the purple mudstone in paleosol of Figure 3 (combined plane and reflected light). **C)** Field photo of yellow-brown (goethite) masses (arrows) within gray rhizohaloes. Purple mudstone from an imperfectly to poorly drained paleosol. Scale shows centimeter markings. **D)** Close-up of rhizoliths in Part C showing yellow-brown rhizocretions (arrows) in gray rhizohaloes. **E)** Yellow-brown rhizocretions within a gray depletion zone (rhizohalo) in a purple mudstone from an imperfectly to poorly drained paleosol. Scale shows centimeter markings. **F)** Photomicrograph of yellow-brown rhizocretions in poorly drained purple paleosol of Figure 3 (combined plane and reflected light).

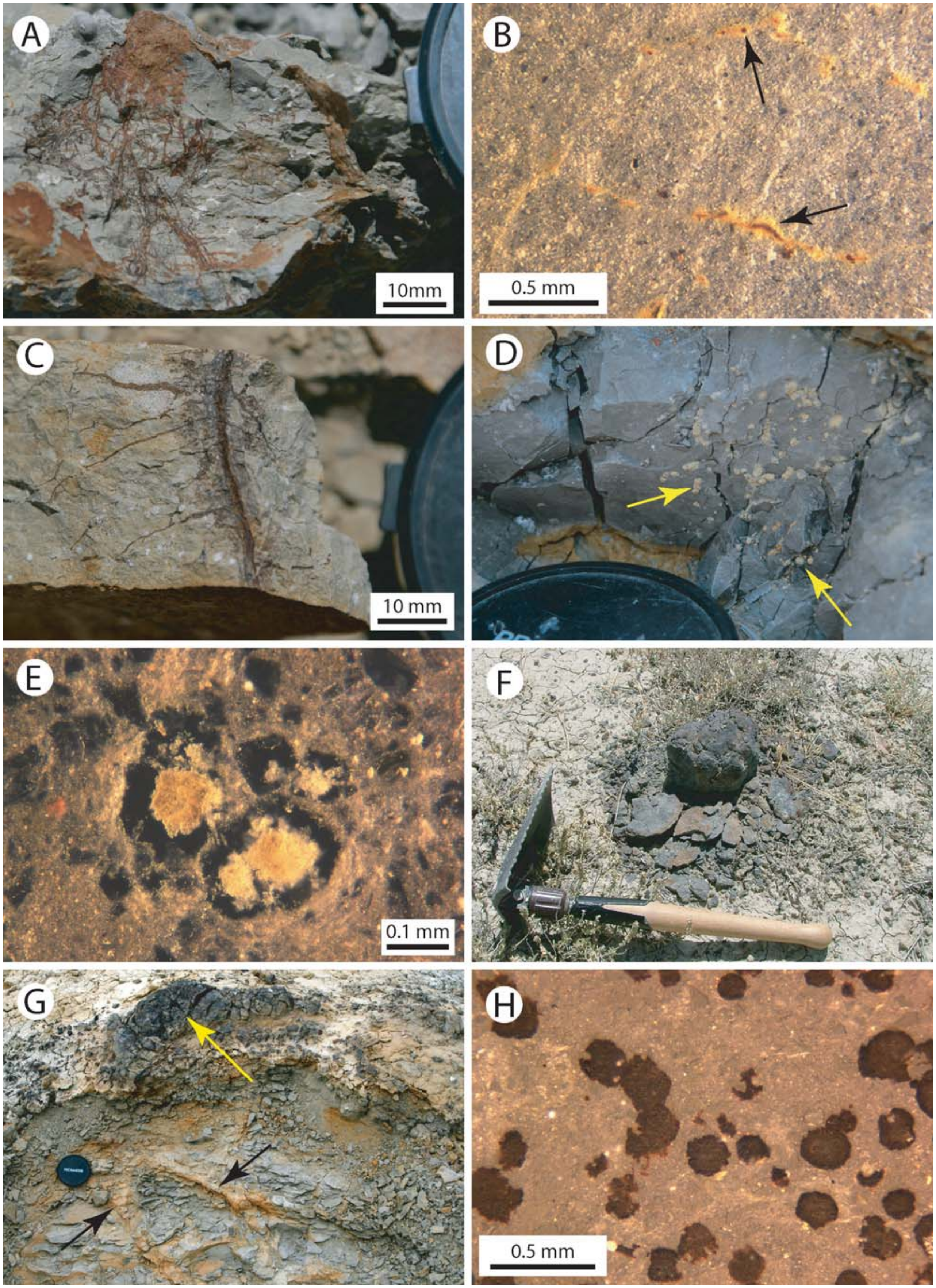
A
10mm
B
0.5 mm
C
10 mm
D
E
0.1 mm
F
G
H
0.5 mm

sub-spherical pores up to 0.25 mm in diameter that contain partially dissolved particles of jarosite (Fig. 7E).

The arrangement of the spheres as branching vermiform features indicates that these are another form of rhizocretion. Jarosite commonly forms from pyrite when drainage of a soil or sediment causes oxidation and subsequent acid conditions (e.g., Van Breeman 1975; Miedema et al. 1986). Other authors have reported pyrite and jarosite associated with modern roots (e.g., Carson et al. 1982; Farrell 1987; Bush et al. 1999), and Hsieh and Yang (1997) found that pyrite accumulation is strongly influenced by root distribution. Rhizoliths preserved with jarosite and pyrite have been described from poorly drained and organic-rich paleosols (e.g., McSweeney and Fastovsky 1987; Bockelie 1994).

The presence of jarosite confirms that at least part of this paleosol was waterlogged most of the year, causing permanently reduced conditions, incomplete decomposition of plant litter, Fe reduction, and pyrite precipitation (e.g., Van Breeman 1975). It is likely that the sulfide concentrations needed to produce the pyrite were generated by the decay of root organic matter, as proposed by Oenema (1990) and Marnette et al. (1993).

The oxidation of the pyrite to form jarosite is probably a relatively recent event related to late Cenozoic exposure of strata in the Bighorn Basin. Paleogene jarosite formation is unlikely because continued sedimentation would have placed the soils ever farther below the groundwater table. Other studies show the presence of jarosite in modern soils that are developing on pyrite-bearing shales (e.g., Carson et al. 1982; Ross et al 1982). In these examples, acidification took place in the modern weathering zone because the pyrite was exposed and oxidized.

Manganiferous Rhizoliths and Sand-Filled Rhizoliths.—Black, nodular bands show at the outcrop surface of the Fort Union Formation paleosols, and disaggregated black nodules weather down the slopes. The nodules are crudely cylindrical in shape with diameters from 12 to 40 cm and preserved lengths up to 40 cm (Fig. 7F). Two black nodules that were excavated have sand-filled tubules extending from them. The better preserved black nodule sits in a gray mudstone. Extending downward from the black nodule are subvertical to subhorizontal tubules that are 2 to 5 cm in diameter and up to 18 cm long. The tubules reach a maximum depth of 12 cm in a dark gray clayey mudstone. In the second example, black nodules are present in a thin bed of sandstone. One excavated example is 18 cm tall and 15 cm in diameter. Sand-filled tubules descend from the nodule and reach a maximum depth of 26 cm in a light olive gray mudstone (Figs. 4B, 7G). Three large, primary tubules that show branching and flattening are preserved. The sand-filled casts have yellow-brown rims indicating the presence of goethite (Fig. 7G). Amber was found in association with one of the black nodules, and leaf-impression fossils were found with another black nodule.

Microprobe analysis of one of the blue-black nodules shows that it contains 77.9 wt % Fe, and XRD analysis shows that the Fe is present as goethite. The nodules also contain MnO (7.75 wt %) and $Si0_2$ (10.5 wt %). Thin sections taken at the transition between a black nodule and the surrounding mudstone matrix show small (0.1–0.2 mm diameter) spheres, which are black in reflected light, scattered through the mudstone matrix (Fig. 7H).

The cylindrical-shaped black nodules and the spreading nature of the associated tubules indicate that these represent *in situ* stump casts of Paleogene trees. The black nodules represent the casts of stumps and primary, surface root systems; the sand-filled tubules are the rhizoliths of the subterranean root system. The color and compositional analysis of the black nodules are consistent with a mix of goethite and Mn-oxides. Manganese accumulations are common in soils, and their color is generally related to the relative amounts of Fe and Mn. For example, brown accumulations tend to be much higher in Fe and black accumulations tend to have increased Mn (e.g., Zhang and Karathanasis 1997).

Manganese oxides are more typical of silt-rich or clay-rich soils with impeded drainage such that soil conditions alternate between reducing and oxidizing (e.g., Birnie and Paterson 1991; Kampf et al. 2000; Stiles et al. 2001). In a study of poorly drained soils in Oregon, Lynn and Austin (1998) found the densest accumulation of Mn-rich nodules in a poorly drained, but not the most poorly drained, soil. Similarly, Schwertmann and Fanning (1976) found Mn-rich nodules to be present in wet but not extremely wet soils. Microorganisms are considered to be important in precipitating ferromanganese materials (e.g., Konhauser 1998; Kampf et al. 2000), and roots may promote nodule formation by providing a ready source of carbon for the bacteria (Robbins et al. 1992). Consequently, the association of Mn oxides with the stump casts is reasonable.

Rhizoliths preserved as sandstone molds have been described by other authors (e.g., McSweeney and Fastovsky 1987; Driese et al. 1997; McCarthy et al. 1998). McCarthy et al. (1998), for example, described tubular sandstone molds up to 15 cm in diameter and 40 cm long that bifurcate downwards into smaller tubes. The sandstone tubes have a thin coating of Fe or Mn oxides.

SIGNIFICANCE FOR PALEODRAINAGE

Gray rhizohaloes with red or purple hypocoatings are characteristic of the moderately well-drained red paleosols. The nature of the rhizohalo and color (as a proxy for mineralogy) of the Fe-oxide rim provide information about the intensity of the gleying that a paleosol underwent. Weak development of both the rhizohalo and the rim indicates incipient gleying. With continued gleying, the bleached zone enlarged and the red rims intensified. Eventually, the Fe-oxide rim consists of a purple inner ring and an outer red ring, and finally only a purple rim remains around the rhizohalo.

Gray rhizohaloes are common also in the imperfectly to poorly drained purple paleosols; however, the hypocoatings are yellow-brown (goethite) rather than hematitic (red) and can form rhizotubules. Rhizoliths with carbonaceous material, preserved as yellow-brown tendrils or rhizocretions, are present but sparse in well-drained paleosols. Those features are more typical of more poorly drained paleosols.

Calcareous rhizocretions—either calcareous, tubular concretions or micro-accumulations of carbonate within gray rhizotubules—are common in the moderately well-drained red paleosols. Although tubular rhizocretions are absent from the poorly drained purple paleosols, micro-accumulations of carbonate are present in gray rhizohaloes, but they are rare. Previously, Kraus (2002) documented carbonate micro-accumulations in rhizoliths preserved as gray depletion zones in paleosols that

←

FIG. 7.—Rhizoliths and root fossils in very poorly drained paleosols. **A)** Field photo of yellow-brown rhizocretions of fine roots in gray paleosol shown in Figure 4. **B)** Photomicrograph of branching, yellow-brown rhizoliths that locally contain red areas (arrows) that indicate hematite (combined plane and reflected light). **C)** Field photo of black carbonaceous root fossils in gray matrix of a very poorly drained paleosol. Primary root gives rise to first-order and second-order lateral root fossils. **D)** Field photo showing jarosite spheres (arrows) arranged as branching, vermiform features interpreted as rhizocretions. **E)** Photomicrograph of partly preserved jarosite spheres in paleosol matrix (reflected light). **F)** Field photo of crudely cylindrical, black nodule situated in a gray mudstone. **G)** Field photo of manganiferous nodule (yellow arrow) from which sand-filled tubules (black arrows) descend in a light olive gray mudstone. The sand-filled casts have yellow-brown rims. **H)** Photomicrograph of small black spheres scattered through the mudstone at the margin between a manganiferous nodule and its containing matrix (reflected light).

contain both a purple and a red mudstone and that appear to be intermediate in drainage between the red and the purple paleosols.

Rhizocretions preserved as yellow-brown (goethite) accumulations or tendrils within gray rhizohaloes are common in imperfectly to poorly drained paleosols. These rhizoliths formed in paleosols developed in wetlands that remained poorly drained and anoxic for most of the time. The filamentous, goethitic rhizocretions indicate that roots were oxidized microenvironments (e.g., Brady and Weil 1999). The presence of carbonaceous material associated with some of these rhizoliths indicates that O_2 was no longer present in the aerenchyma after the root died, allowing the organic carbon to be preserved.

Black, lignitic strands representing actual root fossils are found in all of the paleosols; however, their abundance and mode of occurrence vary with soil drainage. Carbonaceous root fossils are much more common in very poorly drained paleosols, and they are found in the gray matrix, although yellow-brown goethite accumulations are associated with some lignitic root material. Preservation of the lignitic strands is strongly related to soil drainage conditions. The highest relative number of most lignitic strands occurs in poorly drained paleosols and the least in moderately drained paleosols. Within poorly to imperfectly drained paleosols they are found generally within gray depletion zones (e.g., Fig. 7A).

The presence of Mn-rich stump casts in some of the gray paleosols in the Willwood Formation and rhizoliths preserved in other gray paleosols suggests that small- to large-diameter trees grew in poorly to very poorly drained paleosols. The reduced matrix color, the presence of amber, the carbonaceous leaf-compression fossils, and the high density of rhizocretions and associated shallow rhizoliths suggest this was an area similar to present-day hardwood-forest swamps with saturated soils and seasonal standing water. This Willwood paleoenvironment likely experienced a sudden and permanent rise in water table, possibly associated with avulsion of the channel, permanently drowning the forest. This resulted in the precipitation of ferromanganese minerals in the woody tissue of the trunks and surface root system, as well as precipitation of yellow-brown (goethite) hypocoatings on the shallow root system.

CONCLUSIONS

(1) Paleosols that range from moderately well drained to very poorly drained characterize the Willwood and Fort Union formations in the McDermotts Butte area of the Bighorn Basin.

(2) The different paleosols are distinguished by different kinds of rhizoliths. In particular, the mineralogy of the rhizoliths varies according to paleosol drainage. The better drained red paleosols are typified by carbonate-bearing rhizoliths and iron-depleted rhizohaloes with hematitic rims. Imperfectly to poorly drained paleosols have rhizoliths preserved with goethite, and the very poorly drained paleosols are more likely to have preservation of carbonaceous root fossils and Mn-enriched rhizoliths.

(3) The term rhizohalo is introduced to describe root trace fossils with a core that is depleted of Fe and an outer rim enriched in Fe oxides. Without the color variations caused by Fe depletion and enrichment, these rhizoliths would be difficult to observe in the paleosols.

(4) The results presented here show that careful analysis of rhizoliths, which are common in paleosols, can help produce a clearer and more thorough interpretation of past soil drainage. Information about ancient soil moisture regimes is important for understanding past climatic conditions in continental settings and for reconstructing terrestrial paleolandscapes (e.g., Kraus 1999). Rhizoliths and root fossils contain valuable information that can greatly augment the paleoenvironmental interpretive strength of continental deposits.

ACKNOWLEDGMENTS

M.J.K. acknowledges support from National Science Foundation Grants EAR-0000616 and 0228858. S.T.H. acknowledges support from National Science Foundation Grant EAR-02293000. We thank reviewers Cynthia Stiles and David Ufnar and Associate Editor Paul McCarthy for constructive reviews that improved the original manuscript.

REFERENCES

Aslan, A., and Autin, W.J., 1998, Holocene flood-plain soil formation in the southern lower Mississippi Valley: implications for interpreting alluvial paleosols: Geological Society of America, Bulletin, v. 110, p. 433–449.

Bao, H., Koch, P.L., and Rumble, D., III, 1999, Paleocene–Eocene climatic variation in western North America: evidence from the $\delta^{18}O$ of pedogenic hematite: Geological Society of America, Bulletin, v. 111, p. 1405–1415.

Berner, R.A., 1984, Sedimentary pyrite formation; an update: Geochimica et Cosmochimica Acta., v. 48, p. 605–615.

Birnie, A.C., and Paterson, E., 1991, The mineralogy and morphology of iron and manganese oxides in an imperfectly-drained Scottish soil: Geoderma, v. 50, p. 219–237.

Blodgett, R.H., 1988, Calcareous paleosols in the Triassic Dolores Formation, southwestern Colorado, *in* Reinhardt, J., and Sigleo, W.R., eds., Paleosols and Weathering Through Geologic Time: Geological Society of America, Special Paper 216, p. 103–121.

Blodgett, R.H., Crabaugh, J.P., and McBride, E.F., 1993, The color of red beds—a geologic perspective, *in* Bigham, J.M., and Ciolkosz, E.J., eds., Soil Color: Madison, Wisconsin, Soil Science Society of America, p. 127–159.

Bockelie, J.F., 1994, Plant roots in core, *in* Donovan, S.K., ed., The Palaeobiology of Trace Fossils: Baltimore, Maryland, The Johns Hopkins University Press, p. 177–199.

Bown, T.M., 1980, Summary of latest Cretaceous and Cenozoic sedimentary, tectonic, and erosional events, Bighorn Basin, Wyoming, *in* Gingerich, P.D., ed., Early Cenozoic Paleontology and Stratigraphy of the Bighorn Basin, Wyoming: University of Michigan, Papers on Paleontology 24, p. 5–32.

Brady, N.C., and Weil, R.R., 1999. Elements of the Nature and Properties of Soils: Upper Saddle River, New Jersey, Prentice Hall, 559 p.

Bullock, P., Fedoroff, N., Jongerius, A., Stoops, G., and Tursina, T., 1985. Handbook for Soil Thin Section Description: Wolverhampton, England, Waine Research Publications, 152 p.

Bush, R.T., and Sullivan, L.A., 1999, Pyrite micromorphology in three Australian Holocene sediments: Australian Journal of Soil Research, v. 37, p. 637–654.

Carson, C.D., Fanning, D.S., and Dixon, J.B., 1982, Alfisols and Ultisols with acid sulfate weathering features in Texas, *in* Kittrick, J.A., Fanning, D.S., and Hossner, L.R., eds., Acid Sulfate Weathering: Soil Science Society of America, Special Publication 10, p. 127–146.

Cohen, A.S., 1982, Paleoenvironments of root casts from the Koobi Fora Formation, Kenya: Journal of Sedimentary Petrology, v. 52, p. 401–414.

Cornell, R.M., and Schwertmann, U., 1979, Influence of organic anions on the crystallization of ferrihydrite: Clays and Clay Minerals, v. 27, p. 402–410.

Cornell, R.M., and Schwertmann, U., 2003. The Iron Oxides: Structure, Properties, Reactions, Occurrences, and Uses: Weinheim, Wiley-VCH, 664 p.

Curl, E.A., and Truelove, B., 1986. The Rhizosphere: Berlin, Springer-Verlag, 288 p.

Davies-Vollum, K.S., 2001, Not just red beds: the occurrence and formation of drab sections in the Willwood Formation of the Bighorn Basin, *in* Gingerich, P.D., ed., Paleocene–Eocene Stratigraphy and Biotic Change in the Bighorn and Clarks Fork Basins, Wyoming: University of Michigan, Papers on Paleontology 33, p. 29–35.

Dent, D., 1986, Acid Sulphate Soils: A Baseline for Research and Development: Wageningen, The Netherlands, International Institute for Land Reclamation and Improvements, Publication 39, 204 p.

Driese, S.G., Mora, C.I., and Elick, J.M., 1997, Morphology and taphonomy of root and stump casts of the earliest trees (Middle to Late Devonian), Pennsylvania and New York, USA: Palaios, v. 12, p. 524–537.

Duchaufour, P., 1982, Pedology: London, George Allen & Unwin Ltd., 448 p.

Ekdale, A.A., Bromley, R.G., and Pemberton, S.G., 1984, Ichnology: The Use of Trace Fossils in Sedimentology and Stratigraphy: SEPM, Short Course Notes 15, 317 p.

Elick, J.M., Driese, S.G., and Mora, C.I., 1998, Very large plant and root traces from the Early to Middle Devonian: implications for early terrestrial ecosystems and atmospheric $p(CO_2)$: Geology, v. 26, p. 143–146.

Fanning, D.S., and Fanning, M.C.B., 1989, Soil: Morphology, Genesis, and Classification: New York, John Wiley & Sons, 395 p.

Farrell, K.M., 1987, Sedimentology and facies architecture of overbank deposits of the Mississippi River, False River Region, Louisiana, *in* Ethridge, F.G., Flores, R.M., and Harvey, M.D., eds., Recent Developments in Fluvial Sedimentology: SEPM, Special Publication 39, p. 111–120.

Griffin, R.W., Wilding, L.P., and Drees, L.R., 1992, Relating morphological properties to wetness conditions in the Gulf Coast Prairie of Texas, *in* Kimble, J.J., ed., Proceedings of the Eighth International Soil Correlation Meeting (VIII ISCOM): Characterization, Classification, and Utilization of Wet Soils: U.S. Department of Agriculture, Soil Conservation Service, National Soil Survey Center, p. 126–134.

Hasiotis, S.T., 2002. Continental Trace Fossils: SEPM, Short Course Notes 51, 130 p.

Hasiotis, S.T., 2004, Reconnaissance of Upper Jurassic Morrison Formation ichnofossils, Rocky Mountain region, USA: environmental, stratigraphic, and climatic significance of terrestrial and freshwater ichnocoenoses: Sedimentary Geology, v. 167, p. 277–368.

Hasiotis, S.T., and Mitchell, C.E., 1993, A comparison of crayfish burrow morphologies: Triassic and Holocene fossil, paleo- and neo-ichnological evidence, and the identification of their burrowing signatures: Ichnos, v. 2, p. 291–314.

Hsieh, Y.P., and Yang, C.H., 1997, Pyrite accumulation and sulfate reduction as affected by root distribution in a *Juncus* (needle rush) salt marsh: Estuaries, v. 20, p. 640–645.

Kampf, N., and Schwertmann, U., 1982, Goethite and hematite in a climosequence in southern Brazil and their application in classification of kaolinitic soils: Geoderma, v. 29, p. 27–39.

Kampf, N., Scheinost, A.C., and Schulze, D.G., 2000, Oxide minerals, *in* Sumner, M.E., ed., Handbook of Soil Sciences: Boca Raton, Florida, CRC Press, p. F125–168.

Kennett, J.P., and Stott, L.D., 1991, Abrupt deep sea warming, paleoceanographic changes and benthic extinctions at the end of the Paleocene: Nature, v. 353, p. 319–322.

Klappa, C.F., 1980, Rhizoliths in terrestrial carbonates: classification, recognition, genesis, and significance: Sedimentology, v. 26, p. 613–629.

Konhauser, K.O., 1998, Diversity of bacterial iron mineralization: Earth-Science Reviews, v. 43, p. 91–121.

Kraus, M.J., 1998, Development of potential acid sulfate paleosols in Paleocene floodplains, Bighorn Basin, Wyoming, USA: Palaeogeography, Palaeoclimatology, Palaeoecology, v. 144, p. 203–224.

Kraus, M.J., 1999, Paleosols in clastic sedimentary rocks: their geologic applications: Earth-Science Reviews, v. 47, p. 41–70.

Kraus, M.J., 2002, Basin-scale changes in floodplain paleosols: implications for interpreting alluvial architecture: Journal of Sedimentary Research, v. 72, p. 500–509.

Kraus, M.J., and Aslan, A., 1993, Eocene hydromorphic paleosols: significance for interpreting ancient floodplain processes: Journal of Sedimentary Petrology, v. 63, p. 453–463.

Landon, J.R., 1984. Booker Tropical Soil Manual: Bath, Great Britain, Booker Agricultural International Limited, 450 p.

Lynn, W., and Austin, W., 1998, Oxymorphic manganese (iron) segregations in a wet soil catena in the Willamette Valley, Oregon, *in* Rabenhorst, M.C., Bell, J.C., and McDaniel, P.A., eds., Quantifying Soil Hydromorphology: Soil Science Society of America, Special Publication 54, p. 209–226.

Macedo, J., and Bryant, R.B., 1987, Morphology, mineralogy, and genesis of a hydrosequence of Oxisols in Brazil: Soil Science Society of America, Journal, v. 51, p. 690–698.

Macedo, J., and Bryant, R.B., 1989, Preferential microbial reduction of hematite over goethite in a Brazilian Oxisol: Soil Science Society of America, Journal, v. 53, p. 1114–1118.

Marnette, E.C.L., Van Breeman, N., Hordijk, K.A., and Cappenberg, T.E., 1993, Pyrite formation in two freshwater systems in the Netherlands: Geochimica et Cosmochimica Acta, v. 57, p. 4165–4177.

McBride, E.F., 1974, Significance of color in red, green, purple, olive, brown, and gray beds of Difunta Group, northeastern Mexico: Journal of Sedimentary Petrology, v. 44, p. 760–773.

McCabe, P.J., and Parrish, J.T., 1992, Tectonic and climatic controls on Cretaceous coals, *in* McCabe, P.J., and Parrish, J.T., eds., Controls on the Distribution and Quality of Cretaceous Coals: Geological Society of America, Special Paper 267, p. 1–15.

McCarthy, P., Martini, I., and Leckie, D., 1998, Use of micromorphology for palaeoenvironmental interpretation of complex alluvial palaeosols: an example from the Mill Creek Formation (Albian), southwestern Alberta, Canada: Palaeogeography, Palaeoclimatology, Palaeoecology, v. 143, p. 87–110.

McSweeney, K., and Fastovsky, D.E., 1987, Micromorphological and SEM analysis of Cretaceous–Paleogene Petrosols from eastern Montana and western North Dakota: Geoderma, v. 40, p. 49–63.

Miedema, R., Jongmans, A.G., and Slaga, S., 1986, Micromorphological observations on pyrite and its oxidation products in four Holocene alluvial soils in The Netherlands, *in* Stoops, G., and Eswaran, H., eds., Soil Micromorphology: New York, Van Nostrand Reinhold, Soil Series Paper 25, p. 313–337.

Neasham, J.W., and Vondra, C.F., 1972, Stratigraphy and petrology of the lower Eocene Willwood Formation, Bighorn Basin, Wyoming: Geological Society of America, Bulletin, v. 83, p. 2167–2180.

Oenema, O., 1990, Pyrite accumulation in salt marshes in the Eastern Scheldt, southwest Netherlands: Biogeochemistry, v. 9, p. 75–98.

Omar, G.I., Lutz, T.M., and Giegengack, R., 1994, Apatite fission-track evidence for Laramide and post-Laramide uplift and anomalous thermal regime at the Beartooth overthrust, Montana–Wyoming: Geological Society of America, Bulletin, v. 106, p. 74–85.

PiPujol, M.D., and Buurman, P., 1994, The distinction between ground-water gley and surface-water gley phenomena in Tertiary Paleosols of the Ebro Basin, NE Spain: Palaeogeography, Palaeoclimatology, Palaeoecology, v. 110, p. 103–113.

PiPujol, M.D., and Buurman, P., 1997, Dynamics of iron and calcium carbonate redistribution and palaeohydrology in middle Eocene alluvial paleosols of the southeast Ebro Basin margin (Catalonia, northeast Spain): Palaeogeography, Palaeoclimatology, Palaeoecology, v. 134, p. 87–107.

Rabenhorst, M.C., and Haering, K.C., 1989, Soil micromorphology of a Chesapeake Bay tidal marsh: implications of sulfur accumulation: Soil Science, v. 147, p. 339–349.

Ransom, M.D., Smeck, N.E., and Bigham, J.M., 1987, Micromorphology of seasonally wet soils on the Illinoian Till Plain, USA: Geoderma, v. 40, p. 83–99.

Retallack, G.J., 1983, Late Eocene and Oligocene paleosols from Badlands National Park, South Dakota: Geological Society of America, Special Paper 193, 82 p.

Retallack, G.J., 1991, Untangling the effects of burial alteration and ancient soil formation: Annual Review of Earth and Planetary Sciences, v. 19, p. 183–206.

Retallack, G.J., 2001, Soils of the Past: An Introduction to Paleopedology, Second Edition: Oxford, U.K., Blackwell Science, 404 p.

Robbins, E.I., D'Agostino, J.P., Ostwald, J., Fanning, D.S., Carter, V., and Van Hoven, R.L., 1992, Manganese nodules and microbial oxidation of manganese in the Huntley Meadows Wetland, Virginia, USA, *in* Skinner, H.C.W., and Fitzpatrick, R.W., eds., Biomineralization Processes of Iron and Manganese: Catena Supplement 21, p. 179–202.

Ross, G.J., Ivarson, K.C., and Miles, N.M., 1982, Microbial formation of basic ferric sulfates in laboratory systems and in soils, *in* Kittrick, J.A., Fanning, D.S., and Hossner, L.R., eds., Acid Sulfate Weathering: Madison, Wisconsin, Soil Science Society of America, p. 77–94.

Sarjeant, W.A.S., 1975, Plant trace fossils, *in* Frey, R.W., ed., The Study of Trace Fossils: New York, Springer Verlag, p. 163–179.

Scheinost, A.C., and Schwertmann, U., 1999, Color Identification of Iron Oxides and Hydroxysulfates: Use and Limitations: Soil Science Society of America, Journal, v. 63, p. 1463–1471.

Schwertmann, U., 1993, Relations between iron oxides, soil color, and soil formation, *in* Bigham, J.M., and Ciolkosz, E.J., eds., Soil Color: Soil Science Society of America, Special Publication 31, p. 51–69.

Schwertmann, U., and Fanning, D.S., 1976, Iron–manganese concretions in hydrosequences of soils in loess in Bavaria: Soil Science Society of America, Journal, v. 40, p. 731–738.

Schwertmann, U., and Taylor, R.M., 1977, Iron oxides, *in* Dixon, J.B., and Weed, S.B., eds., Minerals in Soil Environments: Madison, Wisconsin, American Society of Agronomy and Soil Science Society of America, p. 145–180.

Schwertmann, U., and Taylor, R.M., 1989, Iron oxides, *in* Dixon, J.B., and Weed, S.B., eds., Minerals in Soil Environments, Second Edition: Madison, Wisconsin, Soil Science Society of America, p. 379–438.

Smith, R.M.H., 1987, Helical burrow casts of therapsid origin from the Beaufort Group (Permian) of South Africa: Palaeogeography, Palaeoclimatology, Palaeoecology, v. 57, p. 285–331.

Sprecher, S.W., 2001, Basic concepts of soil science, *in* Richardson, J.L., and Vepraskas, M.J., eds., Wetland Soils: Boca Raton, Lewis Publishers, p. 3–18.

Stiles, C.A., Mora, C.I., and Driese, S.G., 2001, Pedogenic iron–manganese nodules in Vertisols: A new proxy for paleoprecipitation?: Geology, v. 29, p. 943–946.

Stolt, M.H., Ogg, C.M., and Baker, J.C., 1994, Strongly contrasting redoximorphic patterns in Virginia Valley and Ridge paleosols: Soil Science Society of America, Journal, v. 58, p. 477–484.

Sundby, B., Vale, C., Caçador, I., Catarino, F., Madureira, M.-J., and Caetano, M., 1998, Metal-rich concretions on the roots of salt-marsh plants: Mechanism and rate of formation: Limnology and Oceanography, v. 43, p. 245–252.

Sundby, B., Vale, C., Caetano, M., and Luther, G.W., III, 2003, Redox chemistry in the root zone of a salt marsh sediment in the Tagus Estuary, Portugal: Aquatic Geochemistry, v. 9, p. 257–271.

Van Breeman, N., 1975, Acidification and deacidification of coastal plain soils as a result of periodic flooding: Soil Science Society of America, Proceedings, v. 39, p. 1153–1157.

Van Breeman, N., 1982, Genesis, morphology, and classification of acid sulfate soils in coastal plains, *in* Kittrick, J.A., Fanning, D.S., and Hossner, L.R., eds., Acid Sulfate Weathering: Madison, Wisconsin, Soil Science Society of America, p. 95–108.

Vepraskas, M.J., 1994. Redoximorphic Features for Identifying Aquic Conditions: North Carolina Agricultural Research Service, Technical Bulletin 301, 33 p.

Vepraskas, M.J., Wilding, L.P., and Drees, L.R., 1992, Aquic conditions for soil taxonomy: concepts, soil morphology and micromorphology, *in* Ringrose-Voase, A.J., and Humphreys, G.S., eds., Soil Micromorphology: Studies in Management and Genesis: Amsterdam, Elsevier, p. 117–131.

Violante, A., Barberis, E., Pigna, M., and Boero, V., 2003, Factors affecting the formation, nature, and properties of iron precipitation products at the soil–root interface: Journal of Plant Nutrition, v. 26, p. 1889–1908.

Wilding, L.P., and Tessier, D., 1988, Genesis of Vertisols: shrink–swell phenomena, *in* Wilding, L.P., and Puentes, R., eds., Vertisols: Their Distribution, Properties, Classification and Management: College Station, Texas, Texas A&M University, p. 55–96.

Wing, S.L., 1981, A study of paleoecology and paleobotany in the Willwood Formation (early Eocene, Wyoming) [unpublished Ph.D. Dissertation]: Yale University: New Haven, Connecticut, 416 p.

Wing, S.L., and Greenwood, D.R., 1993, Fossils and fossil climate: the case for equable continental interiors in the Eocene, *in* Allen, J.R.L., Hoskins, B.J., Sellwood, B.W., and Spicer, R.A., eds., Palaeoclimates and their Modelling with Special Reference to the Mesozoic Era: Royal Society (London), Philosophical Transactions, v. 341, p. 243–252.

Wing, S.L., Bao, H., and Koch, P.L., 2000, An early Eocene cool period? Evidence for continental cooling during the warmest part of the Cenozoic, *in* Huber, B.T., Macleod, K.G., and Wing, S.L., eds., Warm Climates in Earth History: Cambridge, U.K., Cambridge University Press, p. 197–237.

Wright, V.P., 1992, Paleosol recognition: a guide to early diagenesis in terrestrial settings, *in* Wolf, K.H., and Chilingarian, G.V., eds., Diagenesis, III: Amsterdam, Elsevier, p. 591–619.

Wright, V.P., Taylor, K.G., and Beck, V.H., 2000, The paleohydrology of Lower Cretaceous seasonal wetlands, Isle of Wight, Southern England: Journal of Sedimentary Research, v. 70, p. 619–632.

Zachos, J.C., Lohmann, K.C., Walker, J.C.G., and Wise, S.W., 1993, Abrupt climate change and transient climates during the Paleogene: A marine perspective: Journal of Geology, v. 101, p. 191–213.

Zhang, M., and Karathanasis, A.D., 1997, Characterization of iron–manganese concretions in Kentucky Alfisols with perched water tables: Clays and Clay Minerals, v. 45, p. 428–439.

Received 23 May 2005; accepted 4 November 2005.